

A New Approach to Design of Dual-band Power Divider Using Admittance Matrix

Yinong Yan, Ting Luo^{*}, Ruifang Su, and Jing Lu

Abstract—A new approach to design of a dual-band power divider with single transmission-line section is proposed in this paper. Apart from the isolation resistor, admittance matrix is used to synthesize the dual-band divider. According to the required admittance matrixes at two frequencies, a modified configuration with shunting open/short stubs at each port is presented. A new compact dual-band power divider (operating at 1.0 GHz and 4.5 GHz) is developed to validate this proposal. Experimental results demonstrate that the return loss is better than 19.2 dB, insertion loss less than 0.59 dB, and isolation better than 23.61 dB at two operation frequencies. The measured relative bandwidths of 15 dB return loss are 35.9% and 12.4% for the lower and higher bands, respectively.

1. INTRODUCTION

Power dividers are widely used in microwave and RF applications. In recent years, the trend of multiband mobile phones promotes the development of dual-band power dividers [1–8]. A conventional Wilkinson power divider operates only at design frequency and its odd harmonics. A dual-band power divider with a simplified two-section transformer was proposed [1], but its outputs return loss and port isolation were poor [2]. In [3] and [4], a new design was realized with ideal response using extra inductor and capacitor connected in parallel with the isolation resistor. But characteristics of lumped elements usually deteriorate properties in high frequency because of parasitic effects. In [5], composite right-/left-handed transmission lines were used to realize dual-band power dividers. However, the proposed configuration was complicated, which increased design and fabrication difficulties. In [6], coupled lines were used to realize a dual-band power divider. However, the relative bandwidth of 15 dB return loss was narrow. The power dividers in [7] still suffered from large size. Moreover, frequency ratio in previous works is small which limits the applications in some multi-band systems such as the fourth generation mobile communication systems. Frequency ratios in [8] were large, but the extra lumped elements used decreased their performance in high frequencies. Besides, two-section transformer means large circuit's size especially at low frequency.

In this paper, a new approach to design of a dual-band power divider is presented. It uses single transmission-line section and does not include extra lumped components. Based on the admittance matrix, closed-form design equations are derived. For verification, a new dual-band (1.0 GHz and 4.5 GHz) power divider is shown. The main features of the proposed power divider are: 1) only single transmission-line section is used; 2) no other extra lumped component is used except the isolation resistor; 3) wide range of frequency ratios m is implemented; 4) closed-form design equations are deduced. The method proposed in this work simplifies the design of a dual-band power divider.

Received 31 December 2016, Accepted 8 February 2017, Scheduled 3 March 2017

^{*} Corresponding author: Ting Luo (luotingky@163.com).

The authors are with the College of Science and Technology, Ningbo University, Ningbo 315211, China.

2. DUAL-BAND POWER DIVIDER THEORY

Power divider is a three-port network with one input (port 1) and two outputs (port 2 and port 3). All ports are matched ($S_{ii} = 0$, $i = 1, 2, 3$), and two outputs are isolated ($S_{23} = 0$). For the equal-split case with θ phase shift, its scatter-matrix can be expressed as:

$$S = \frac{\sqrt{2}e^{-j\theta}}{2} \begin{bmatrix} 0 & 1 & 1 \\ 1 & 0 & 0 \\ 1 & 0 & 0 \end{bmatrix} \quad (1)$$

The conversion of scatter-matrices to admittance matrices is as follows:

$$Y = (U - S)(U + S)^{-1} / Z_0 \quad (2)$$

where Z_0 is the port impedance and U the unit matrix.

So, the admittance matrix of a power divider with θ phase shift is:

$$Y = \frac{1}{Z_0} \begin{bmatrix} -j \cot \theta & j \frac{\sqrt{2}}{2 \sin \theta} & j \frac{\sqrt{2}}{2 \sin \theta} \\ j \frac{\sqrt{2}}{2 \sin \theta} & \frac{1}{2} - \frac{j}{2} \cot \theta & -\frac{1}{2} - \frac{j}{2} \cot \theta \\ j \frac{\sqrt{2}}{2 \sin \theta} & -\frac{1}{2} - \frac{j}{2} \cot \theta & \frac{1}{2} - \frac{j}{2} \cot \theta \end{bmatrix} \quad (3)$$

For dual-band operation, let f_1 and $f_2 = mf_1$ (assuming that the frequency ratio is an arbitrary rational number larger than 1) be the lower and upper band frequencies, respectively, and let θ_1 and θ_2 be the phase shifts corresponding to the two frequencies. To simplify the design, it is better that the mutual admittance between port 2 and port 3 is a pure real number, so $\theta_1 = \pi/2$, $\theta_2 = -\theta_1 = -\pi/2$ are selected. And the admittance matrix at the two frequencies can be expressed as:

$$Y_i = \begin{bmatrix} 0 & \frac{(-1)^{i+1}j}{\sqrt{2}Z_0} & \frac{(-1)^{i+1}j}{\sqrt{2}Z_0} \\ \frac{(-1)^{i+1}j}{\sqrt{2}Z_0} & \frac{1}{2} & -\frac{1}{2} \\ \frac{(-1)^{i+1}j}{\sqrt{2}Z_0} & -\frac{1}{2} & \frac{1}{2} \end{bmatrix} \quad i = 1, 2 \quad (4)$$

From Eq. (4), it can be seen that $Y_1(2, 3) = Y_2(2, 3)$, and it is a pure real number, so the nets between port 2 and port 3 can be realized by a resistor.

The configuration in dashed frame of Fig. 1 is a conventional Wilkinson power divider. Its admittance matrix can be expressed as:

$$Y_{con} = \begin{bmatrix} -j \frac{2 \cot \varphi}{Z} & \frac{j}{Z \sin \varphi} & \frac{j}{Z \sin \varphi} \\ \frac{j}{Z \sin \varphi} & \frac{1}{R} - j \frac{\cot \varphi}{Z} & -\frac{1}{R} \\ \frac{j}{Z \sin \varphi} & -\frac{1}{R} & \frac{1}{R} - j \frac{\cot \varphi}{Z} \end{bmatrix} \quad (5)$$

From Eq. (5) it can be seen that the imaginary parts of $Y_{con}(1, 1)$, $Y_{con}(2, 2)$, and $Y_{con}(2, 3)$ are not equal to zero when the electrical length φ of the two transmission lines is not equal to 90° . Therefore, the conventional power divider is no longer available for Eq. (4). A modified configuration with shunting short/open stubs at each port is proposed. The new configuration is shown in Fig. 1, where Y_a and Y_b are the input admittances looking to the arrows of the short/open stubs; Z_a and Z_b are their characteristic impedances; φ_a and φ_b are their electrical lengths.

The admittance matrix of the proposed power divider can be expressed as [7, 8]:

$$Y_M = \begin{bmatrix} Y_a - j \frac{2 \cot \varphi}{Z} & \frac{j}{Z \sin \varphi} & \frac{j}{Z \sin \varphi} \\ \frac{j}{Z \sin \varphi} & \frac{1}{R} - j \frac{\cot \varphi}{Z} + Y_b & -\frac{1}{R} \\ \frac{j}{Z \sin \varphi} & -\frac{1}{R} & \frac{1}{R} - j \frac{\cot \varphi}{Z} + Y_b \end{bmatrix} \quad (6)$$

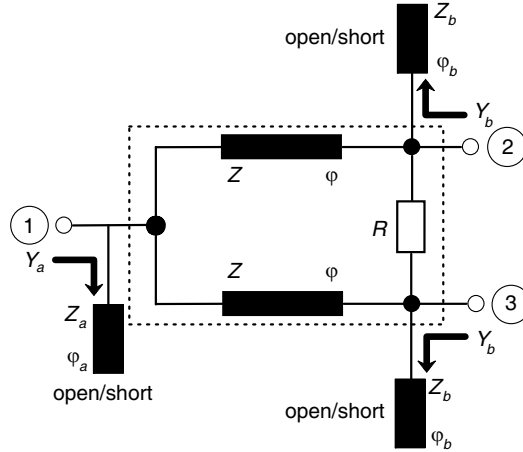


Figure 1. Configuration of the proposed power divider.

where

$$Y_a = \begin{cases} -j \cot \varphi_a / Z_a & \text{short stub} \\ j \tan \varphi_a / Z_a & \text{open stub} \end{cases} \quad (7)$$

$$Y_b = \begin{cases} -j \cot \varphi_b / Z_b & \text{short stub} \\ j \tan \varphi_b / Z_b & \text{open stub} \end{cases} \quad (8)$$

So in frequency f_1 and f_2 , the admittance matrixes are as follows:

$$Y_{Mi} = \begin{bmatrix} Y_{ai} - j \frac{2 \cot \varphi_i}{Z_i} & \frac{j}{Z_i \sin \varphi_i} & \frac{j}{Z_i \sin \varphi_i} \\ \frac{j}{Z_i \sin \varphi_i} & \frac{1}{R} - j \frac{\cot \varphi_i}{Z_i} + Y_{bi} & -\frac{1}{R} \\ \frac{j}{Z_i \sin \varphi_i} & -\frac{1}{R} & \frac{1}{R} - j \frac{\cot \varphi_i}{Z_i} + Y_{bi} \end{bmatrix} \quad i = 1, 2 \quad (9)$$

Let $Y_{M1} = Y_1$ and $Y_{M2} = Y_2$, and the following equations can be derived:

$$Y_{a1} - j \frac{2 \cot \varphi_1}{Z_1} = 0 \quad (10)$$

$$Y_{a2} - j \frac{2 \cot \varphi_2}{Z_2} = 0 \quad (11)$$

$$Z_1 \sin \varphi_1 = \sqrt{2} Z_0 \quad (12)$$

$$Z_2 \sin \varphi_2 = -\sqrt{2} Z_0 \quad (13)$$

$$\frac{1}{R} - j \frac{\cot \varphi_1}{Z_1} + Y_{b1} = \frac{1}{2Z_0} \quad (14)$$

$$\frac{1}{R} - j \frac{\cot \varphi_2}{Z_2} + Y_{b2} = \frac{1}{2Z_0} \quad (15)$$

$$R = 2Z_0 \quad (16)$$

Given the dimensions of the microstrip line, the characteristic impedance and electrical length respectively are [1]:

$$Z = \begin{cases} \frac{60}{\sqrt{\epsilon_e}} \ln \left(\frac{8d}{W} + \frac{W}{4d} \right) & \text{for } W/d \leq 1 \\ \frac{120\pi}{\sqrt{\epsilon_e} [W/d + 1.393 + 0.667 \ln(W/d + 1.444)]} & \text{for } W/d > 1 \end{cases} \quad (17)$$

$$\varphi = \beta l = \sqrt{\epsilon_e} k_0 l = \sqrt{\epsilon_e} \frac{2\pi f}{c} l \quad (18)$$

So $Z_2 = Z_1$ and $\varphi_2 = m\varphi_1$, and Equations (12) and (13) lead to:

$$\sin m\varphi_1 = -\sin \varphi_1 \quad (19)$$

So:

$$m\varphi_1 = 2k_1\pi - \varphi_1 \quad k_1 = 1, 2, \dots \quad (20)$$

$$\text{or } m\varphi_1 = l\pi + \varphi_1 \quad l = 1, 3, 5, \dots \quad (21)$$

$$\varphi_1 = \frac{2k_1\pi}{m+1} \quad k_1 = 1, 2, 3, \dots \quad (22)$$

$$\text{or } \varphi_1 = \frac{l\pi}{m-1} \quad l = 1, 3, 5, \dots \quad (23)$$

$$Z_1 = Z_2 = \frac{\sqrt{2}Z_0}{|\sin \varphi_1|} \quad (24)$$

Now, consider for different cases:

1) For the situation of Eq. (22), from Equations (10) and (11), Y_{a1} , Y_{a2} can be expressed as:

$$Y_{a1} = j \frac{2 \cot \varphi_1}{Z_1} \quad (25)$$

$$Y_{a2} = j \frac{2 \cot \varphi_2}{Z_2} = -j \frac{2 \cot \varphi_1}{Z_1} = -Y_{a1} \quad (26)$$

From Equations (14), (15) and (16), Y_{b1} , Y_{b2} can be expressed as:

$$Y_{b1} = j \frac{\cot \varphi_1}{Z_1} \quad (27)$$

$$Y_{b2} = -j \frac{\cot \varphi_1}{Z_1} = -Y_{b1} \quad (28)$$

According to the imaginary parts of Y_{a1} and Y_{b1} , it can be decided to use open or short stubs. If their imaginary parts are greater than zero, open stubs can be used; on the contrary, short microstrip lines are good candidates. From Equations (7), (8), (26) and (28), the following equation can be deduced:

$$\varphi_{a1} = \frac{k_2\pi}{m+1} \quad k_2 = 1, 2, \dots \quad (29)$$

$$\varphi_{b1} = \frac{k_2\pi}{m+1} \quad k_2 = 1, 2, \dots \quad (30)$$

Then Z_a and Z_b can be expressed as:

$$Z_a = \begin{cases} -Z_1 \cot \varphi_{a1} / (2 \cot \varphi_1) & \text{short stub} \\ Z_1 \tan \varphi_{a1} / (2 \cot \varphi_1) & \text{open stub} \end{cases} \quad (31)$$

$$Z_b = \begin{cases} -Z_1 \cot \varphi_{b1} / \cot \varphi_1 & \text{short stub} \\ Z_1 \tan \varphi_{b1} / \cot \varphi_1 & \text{open stub} \end{cases} \quad (32)$$

2) For the situation of Eq. (23), from Equations (10) and (11), Y_{a1} , Y_{a2} can be expressed as:

$$Y_{a1} = j \frac{2 \cot \varphi_1}{Z_1} \quad (33)$$

$$Y_{a2} = j \frac{2 \cot \varphi_2}{Z_2} = j \frac{2 \cot \varphi_1}{Z_1} = Y_{a1} \quad (34)$$

From Equations (14), (15) and (16), Y_{b1} , Y_{b2} can be expressed as:

$$Y_{b1} = j \frac{\cot \varphi_1}{Z_1} \quad (35)$$

$$Y_{b2} = j \frac{\cot \varphi_1}{Z_1} = Y_{b1} \quad (36)$$

From Equations (7), (8), (24) and (36), the following equation can be deduced:

$$\varphi_{a1} = \frac{k_2\pi}{m+1} \quad k_2 = 1, 2, \dots \quad (37)$$

$$\varphi_{b1} = \frac{k_2\pi}{m+1} \quad k_2 = 1, 2, \dots \quad (38)$$

In this situation, Z_a and Z_b can also be expressed as Eqs. (31) and (32).

3. POWER DIVIDER DESIGN

Based on the above analyses, the design procedure is described as follows:

Step 1: According to the given operating frequency f_1 and $f_2 = mf_1$, calculate the two branch-lines electrical length φ_1 at frequency f_1 by Equation (22) or (23);

Step 2: Calculate the two branch-lines characteristic impedance by Equation (24);

Step 3: Calculate Y_{a1} and Y_{b1} by Equations (25) and (27), according to Y_{a1} and Y_{b1} imaginary parts to decide the use of open or short stubs;

Step 4: Calculate the electrical lengths φ_{a1} and φ_{b1} by Equations (29) and (30) or by Equations (37) and (38);

Step 5: Calculate the impedances Z_a and Z_b according to Equations (31) and (32);

Step 6: Calculate the geometric parameters according to the used substrate.

Different m values of double frequency power dividers can be implemented according to above procedure. The isolation resistor is set to 100 Ohm, and the electrical parameters of different m values of the double frequency dividers are listed in Table 1, according to which the appropriate parameters can be selected.

Table 1. The electrical parameters for the dual-band power divider. (S.L means short line; O.L means open line).

| Case1 | $m\varphi_1 = 2k_1\pi - \varphi_1$ | | | $k_1 = 1, 2, \dots$ | | | | |
|-------|------------------------------------|--------|-------|---------------------|-------|-------|-------------|-------|
| m | ϕ_1 | Z_1 | Y_a | ϕ_{a1} | Z_a | Y_b | ϕ_{b1} | Z_b |
| 1.5 | 288 | 74.35. | S.L | 72 | 37.2 | S.L | 72 | 74.4 |
| 2.5 | 308 | 90.4 | S.L | 51.4 | 45.2 | S.L | 51.4 | 90.4 |
| 3.5 | 240 | 81.7 | O.L | 200 | 25.7 | O.L | 200 | 51.4 |
| 4.5 | 65.5 | 77.7 | O.L | 32.7 | 54.7 | O.L | 32.7 | 109. |
| 5.5 | 55.4 | 85.9 | O.L | 27.7 | 32.7 | O.L | 27.7 | 65.4 |

| Case2 | $m\varphi_1 = l\pi + \varphi_1$ | | | $l = 1, 3, 5, \dots$ | | | | |
|-------|---------------------------------|----------|-------|----------------------|-------|-------|-------------|-------|
| m | ϕ_1 | Z_1 | Y_a | ϕ_{a1} | Z_a | Y_b | ϕ_{b1} | Z_b |
| 1.5 | 360 | ∞ | S.L | 72 | 11.5 | S.L | 72 | 23 |
| 2.5 | 120 | 81.7 | S.L | 51.4 | 56.4 | S.L | 51.4 | 112.8 |
| 3.5 | 216 | 120.3 | O.L | 40 | 36.7 | O.L | 40 | 73.4 |
| 4.5 | 51.4 | 90.4 | O.L | 32.7 | 36.4 | O.L | 32.7 | 72.8. |
| 5.5 | 40 | 110 | O.L | 27.7 | 24.2 | O.L | 27.7 | 48.4 |

4. SIMULATED AND MEASURED RESULTS

To validate the proposed design, a new compact dual-band power divider is implemented. The two operating frequencies are chosen to be 1.0 GHz and 4.5 GHz. The developed divider is fabricated on a Rogers 4003 substrate with the relative permittivity of 3.55 and thickness of 0.508 mm. Fig. 2 shows a

Table 2. The geometric parameters for the fabricated divider (D means design).

| $m \backslash D$ | $w1$ (mm) | $w2$ (mm) | $w3$ (mm) | $l1$ (mm) | $l2$ (mm) | $l3$ (mm) |
|------------------|--------------|--------------|--------------|--------------|--------------|--------------|
| 4.5 | 0.975 | 0.5 | 0.27 | 16.9 | 34.08 | 16 |

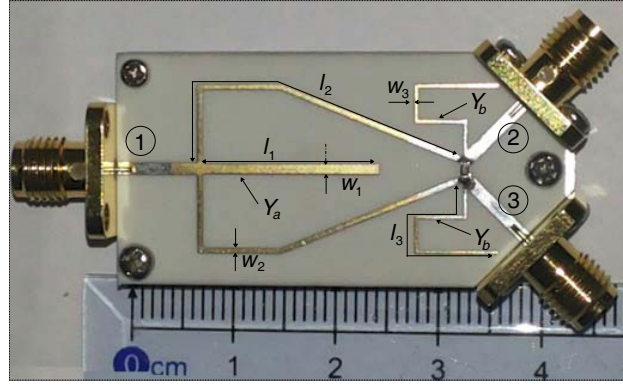


Figure 2. Power divider worked at 1.0 GHz and 4.5 GHz.

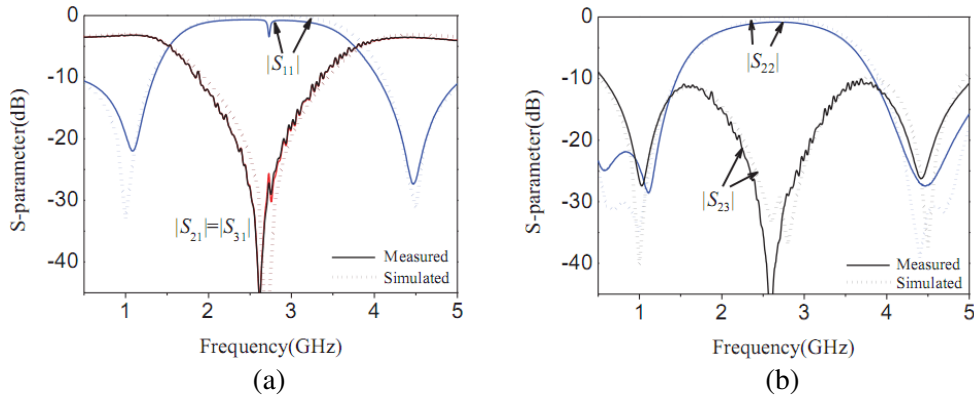


Figure 3. Simulated and measured (a) $|S_{11}|$, $|S_{21}|$, $|S_{31}|$ and (b) $|S_{22}|$, $|S_{23}|$.

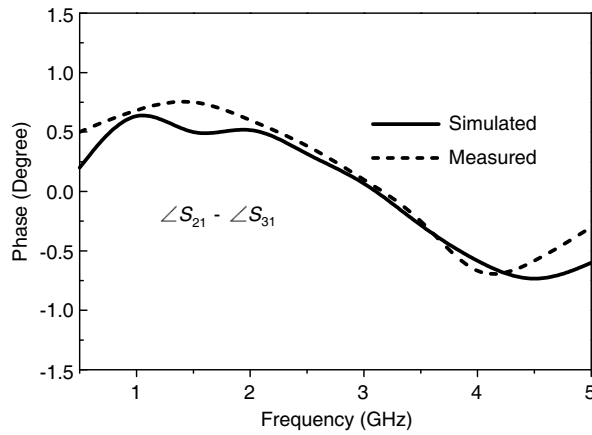


Figure 4. Simulated and measured phase difference between the two output ports.

photograph of the fabricated power divider. The corresponding geometric parameters for this divider are listed in Table 2. The full wave simulator Ansoft HFSS 13.0 has been used. The S -parameter measurements are performed using an Agilent network analyzer, and the measured frequency range is from 0.5 GHz to 5 GHz.

The simulated and measured results are shown in Fig. 3. At the operating frequency of 1.0 GHz, the insertion losses are $|S_{21}| = -3.24$ dB and $|S_{31}| = -3.24$ dB, and the return-losses are $|S_{11}| = -19.27$ dB

and $|S_{22}| = -25.95$ dB. The isolation ($|S_{23}|$) is -26.51 dB, and the 15 dB return loss bandwidth is better than 35.9%. At the operating frequency of 4.5 GHz, the insertion losses are $|S_{21}| = -3.59$ dB and $|S_{31}| = -3.56$ dB, and the return losses are $|S_{11}| = -26.71$ dB and $|S_{22}| = -27.35$ dB. The isolation ($|S_{23}|$) is -23.61 dB, and the 15 dB return loss bandwidth is better than 12.4%. Fig. 4 shows that the $|\angle S_{21} - \angle S_{31}|$ of the phase difference is less than $\pm 1^\circ$ at both passbands. In addition, the proposed structure is relatively simple and realizes wide range of frequency ratios m while keeping small size. A wide bandwidth is achieved at lower frequency, and a modest bandwidth is obtained at higher frequency compared with other structures.

5. CONCLUSION

Admittance matrix is used to synthesize the dual-band power divider in this paper. A new compact dual-band power divider with single transmission-line section is designed and fabricated. It is found that this method can realize large frequency ratio, and the area of the proposed power divider is reduced effectively. The results show that the fabricated power divider agrees well with the proposed theory. It is expected that this proposed design theory for generalized power dividers can find many potential applications in practical circuit designs.

REFERENCES

1. Monzon, C., "A small dual-frequency transformer in two sections," *IEEE Trans. Microw. Theory Tech.*, Vol. 51, No. 4, 1157–1161, Apr. 2003.
2. Srisathit, S., M. Chongcheawchamnan, and A. Worapishet, "Design and realization of dual-band 3 dB power divider based on two-section transmission-line topology," *Electron. Lett.*, Vol. 39, No. 9, 723–724, May 2003.
3. Wu, L., H. Yilmaz, T. Bitzer, A. Pascht, and M. Berroth, "A dual-frequency Wilkinson power divider: For a frequency and its first harmonic," *IEEE Microw. Wireless Compon. Lett.*, Vol. 5, No. 2, 107–109, Feb. 2005.
4. Wu, L., S. Sun, H. Yilmaz, and M. Berroth, "A dual-frequency Wilkinson power divider," *IEEE Trans. Microw. Theory Tech.*, Vol. 54, No. 1, 278–284, Jan. 2006.
5. Bai, Y.-F., X.-H. Wang, C.-J. Gao, X.-W. Shi, and H.-J. Lin, "Compact dual-band power divider using non-uniform transmission line," *Electron. Lett.*, Vol. 47, No. 3, 188–190, Feb. 3, 2011.
6. Liu, Y. C., W. H. Chen, X. Li, and Z. H. Feng, "Design of compact dual-band power dividers with frequency-dependent division ratios based on multisection coupled line," *IEEE Trans. Compon., Packag. Manuf. Technol.*, Vol. 3, No. 3, 467–475, Mar. 2013.
7. Huang, K., S. Zhang, and L. Bei, "A novel symmetrical Wilkinson power divider for dual-band application," *Microwave Comput-Aided Eng.*, Vol. 24, No. 1, 102–108, Jan. 2014.
8. Gao, N. J., G. A. Wu, and Q. H. Tang, "Design of a novel compact dual-band Wilkinson power divider with wide frequency ratio," *IEEE Microw. Wireless Compon. Lett.*, Vol. 24, No. 2, 81–83, Feb. 2015.